Cancer Research

Reciprocal Regulation of DUSP9 and DUSP16 Expression by HIF1 Controls ERK and p38 MAP Kinase Activity and Mediates Chemotherapy-Induced Breast Cancer Stem Cell Enrichment

Haiquan Lu[1,2], Linh Tran[1,2], Youngrok Park[1,2], Ivan Chen[1,2], Jie Lan[1,2,3], Yangyiran Xie[4], and Gregg L. Semenza[1,2,5]

Abstract

Triple-negative breast cancer (TNBC) has a poor prognosis due to its aggressive characteristics and lack of targeted therapies. Cytotoxic chemotherapy may reduce tumor bulk, but leaves residual disease due to the persistence of chemotherapy-resistant breast cancer stem cells (BCSC), which are critical for tumor recurrence and metastasis. Here, we demonstrate that hypoxia-inducible factor (HIF)-1–dependent regulation of mitogen-activated protein kinase (MAPK) signaling pathways contributes to chemotherapy-induced BCSC enrichment. Chemotherapy increased DUSP9 expression and decreased DUSP16 expression in a HIF1–dependent manner, leading to inhibition of ERK and activation of p38 signaling pathways, respectively. Inhibition of ERK caused transcriptional induction of the pluripotency factor Nanog through decreased inactivating phosphorylation of FoxO3, while activation of p38 stabilized Nanog and Klf4 mRNA through increased inactivating phosphorylation of RNA-binding protein ZFP36L1, both of which promoted specification of the BCSC phenotype. Inhibition of HIF1 or p38 signaling blocked chemotherapy-induced pluripotency factor expression and BCSC enrichment. These surprising results delineate a mechanism by which a transcription factor switches cells from ERK to p38 signaling in response to chemotherapy and suggest that therapeutic targeting of HIF1 or the p38 pathway in combination with chemotherapy will block BCSC enrichment and improve outcome in TNBC.

Significance: These findings provide a molecular mechanism that may account for the increased relapse rate of women with TNBC who are treated with cytotoxic chemotherapy and suggest that combining chemotherapy with an inhibitor of HIF1 or p38 activity may increase patient survival. *Cancer Res; 78 (15); 4191–202. ©2018 AACR.*

Introduction

Triple-negative breast cancer (TNBC) is a subtype of breast cancer that lacks expression of the estrogen receptor (ER), progesterone receptor, and human epidermal growth factor receptor 2 (HER2; ref. 1). Compared with other breast cancer subtypes, TNBC is more aggressive with increased risk of recurrence, metastasis, and mortality (2). Cytotoxic chemotherapy, which is the major systemic treatment option for patients with TNBC (3), may dramatically reduce tumor burden but leave behind breast cancer stem cells (BCSC), a small population of residual cancer cells that are resistant to chemotherapy and have infinite proliferative potential and tumor-initiating properties, leading to tumor recurrence and metastasis (4–8). Recently, it has been reported that BCSCs are enriched in response to chemotherapy, which further potentiates the risk of recurrent and metastatic disease (9–12). Therefore, a better understanding of the mechanisms underlying chemotherapy-induced BCSC enrichment is urgently needed.

Cancer cells may develop acquired resistance in response to chemotherapy through a rapid reprogramming of cell signaling (13). The mitogen-activated protein kinase (MAPK) pathways, which control diverse cellular processes including proliferation, differentiation, apoptosis, and metastasis (14), have been implicated in chemoresistance in breast cancer (15). However, little is known about whether alterations of MAPK activities are involved in chemotherapy-mediated BCSC enrichment. The MAPK signaling pathway in mammalian cells includes three classical branches: extracellular signal-regulated kinase (ERK), c-Jun N-terminal kinase (JNK), and p38 MAPK, each of which can be activated by a variety of stimuli, including growth factors, cytokines, and cellular stress (16). We previously reported a molecular mechanism leading to inhibition of MEK, which is the upstream activator of ERK signaling, in BCSCs (11). The activity of MAPKs is tightly regulated by both their kinases and phosphatases. Activation of MAPKs requires phosphorylation of both threonine

[1]Institute for Cell Engineering, Johns Hopkins University School of Medicine, Baltimore, Maryland. [2]McKusick-Nathans Institute of Genetic Medicine, Johns Hopkins University School of Medicine, Baltimore, Maryland. [3]Department of Thoracic Oncology, Cancer Center and State Key Laboratory of Biotherapy, West China Hospital, Sichuan University, Chengdu, China. [4]Krieger School of Arts and Sciences, Johns Hopkins University, Baltimore, Maryland. [5]Departments of Pediatrics, Medicine, Oncology, Radiation Oncology, and Biological Chemistry, Johns Hopkins University School of Medicine, Baltimore, Maryland.

Note: Supplementary data for this article are available at Cancer Research Online (http://cancerres.aacrjournals.org/).

Corresponding Author: Gregg L. Semenza, Johns Hopkins University School of Medicine, 733 N. Broadway, Suite 671, Baltimore, MD 21205. Fax: 443-287-5618; E-mail: gsemenza@jhmi.edu

doi: 10.1158/0008-5472.CAN-18-0270

and tyrosine residues of a conserved T-X-Y motif in the kinase domain, which is catalyzed by MAPK kinases (MKK). Dual-specificity phosphatases (DUSP), which are the major negative regulators of MAPKs, selectively dephosphorylate the T-X-Y motif of their substrates (17). Although less well studied than MKKs, DUSPs are now considered pivotal in regulating the duration and intensity of MAPK activation. DUSPs have much greater enzymatic activity (100–1,000 times) compared with MKKs, because dephosphorylation is a direct reaction without a requirement for ATP (18).

The dynamic regulation of DUSPs makes them appealing targets for controlling MAPK-dependent responses to therapeutics (19). The expression and activity of DUSPs are regulated transcriptionally, posttranscriptionally, and posttranslationally. At the transcriptional level, the expression of DUSPs is regulated by many different transcription factors including AP-1 (20), CREB (21), ETS-1 (22), and NF-κB (23). Recent studies have found that the expression of several DUSPs, such as DUSP2 and DUSP6, is modulated in response to reduced O_2 availability through the activity of hypoxia-inducible factors (HIF; refs. 24, 25), which are master regulators of O_2 homeostasis (26). HIFs are heterodimeric transcription factors consisting of an O_2-regulated HIF1α or HIF2α subunit and a constitutively expressed HIF1β subunit (27). Although intratumoral hypoxia is the major cause of increased HIF activity in human tumors (27, 28), HIF1α and HIF2α mRNA and protein expression are induced in cancer cells exposed to chemotherapy (29), leading to the expression of multiple HIF target genes that are required for chemotherapy-induced BCSC enrichment, as demonstrated by both genetic and pharmacologic loss-of-function studies (10–12). In this study, we found that two DUSP family members, DUSP9 and DUSP16, are reciprocally regulated by HIF1 and contribute to chemotherapy-induced BCSC enrichment through inactivation of ERK and activation of p38 MAPK signaling pathways.

Materials and Methods

Cell culture

MDA-MB-231 and SUM-159 cells were obtained from Dr. Sara Sukumar, Johns Hopkins University School of Medicine in 2011 and were authenticated by STR analysis. PCR-based mycoplasma testing was performed by the Johns Hopkins Genetics Resources Core Facility on an annual basis. MDA-MB-231 cells were maintained in DMEM, and SUM-159 cells were maintained in DMEM/F12 (50:50), both of which were supplemented with 10% fetal bovine serum and 1% penicillin–streptomycin. Cells were maintained at 37°C in a 5% CO_2, 95% air incubator (20% O_2). For hypoxic exposure, cells were placed in a modular incubator chamber (Billups–Rothenberg) that was flushed with a 1% O_2/5% CO_2/94% N_2 gas mixture. All chemicals are listed in Supplementary Table S1.

Lentivirus transduction

Expression vectors encoding short hairpin RNA (shRNA) targeting HIF1α and HIF2α were described previously (30). pLKO.1-puro lentiviral vectors encoding shRNA targeting DUSP9, DUSP16, REST, RCOR2, and ZFP36L1 were purchased from Sigma-Aldrich, and shRNA sequences are shown in Supplementary Table S2. Empty pLx304 vector was purchased from Addgene and pLx304 vector encoding DUSP16 was purchased from DNASU. Lentiviruses were packaged in 293T cells; MDA-MB-231 and SUM-159 cells were transduced and subjected to selection as described previously (12).

Immunoblot assay

Cell lysates from cultured cells were prepared in modified RIPA buffer, whereas cell lysates from tumor tissues were prepared by boiling in 1% SDS. Proteins were separated by SDS-PAGE, blotted onto nitrocellulose membranes, and probed with primary antibodies (Supplementary Table S3). The membranes were then probed with HRP-conjugated secondary antibodies (GE Healthcare) and the chemiluminescent signal was detected using ECL Plus (GE Healthcare).

Reverse transcription and quantitative PCR

Total RNA was extracted with TRIzol (Invitrogen), precipitated with isopropanol, and treated with DNase (DNA-free, Invitrogen). cDNA was synthesized (cDNA reverse transcription kit, Applied Biosystems) and qPCR analysis was performed using SYBR Green and the CFX96 Touch real-time PCR detection system (Bio-Rad). The expression of each target mRNA relative to 18S rRNA was calculated based on the cycle threshold (C_t) as $2^{-\Delta(\Delta C_t)}$, in which $\Delta C_t = C_t$ (target) – C_t (18S rRNA), and $\Delta(\Delta C_t) = \Delta C_t$ (test sample) – ΔC_t (control sample). Primer sequences are shown in Supplementary Table S4.

Chromatin immunoprecipitation assay

MDA-MB-231 cells were cross-linked in 3.7% formaldehyde for 15 minutes, quenched in 0.125 mol/L glycine for 5 minutes and lysed with SDS lysis buffer. Chromatin was sheared by sonication, sonicated lysates were precleared with salmon sperm DNA/protein A agarose slurry (Millipore) for 1 hour and incubated with IgG or antibodies against HIF1α (Santa Cruz Biotechnology), HIF1β, or REST (Novus Biologicals) in the presence of agarose beads overnight. After sequential washing of the agarose beads, DNA was eluted in 1% SDS/0.1 mol/L $NaHCO_3$, and crosslinks were reversed by the addition of 0.2 mol/L NaCl. DNA was purified by phenol-chloroform extraction and ethanol precipitation, and candidate binding sites were analyzed by qPCR. Primer sequences are shown in Supplementary Table S5.

Aldehyde dehydrogenase assay

The aldehyde dehydrogenase (ALDH) assay was performed according to the manufacturer's instructions (Aldefluor, Stem Cell Technologies). Cultured cells were trypsinized, whereas tumor tissues were minced, digested with 1 mg/mL type 1 collagenase (Sigma-Aldrich) at 37°C for 30 minutes, and filtered through a 70-μm cell strainer. A total of 1×10^6 cells were suspended in assay buffer containing 1 μmol/L BODIPY-aminoacetaldehyde and incubated at 37°C for 45 minutes. An aliquot of cells from each sample was treated with 50 mmol/L diethylaminobenzaldehyde (ALDH inhibitor) as a negative control for gating. Samples were subjected to flow cytometry analysis using FACScalibur (BD Biosciences).

Mammosphere assay

Cultured cells were trypsinized, whereas tumor tissues were minced, digested with 1 mg/mL type 1 collagenase (Sigma-Aldrich) at 37°C for 30 minutes, and filtered through a 70-μm cell strainer. The numbers of live cells were determined

using trypan blue staining. Single-cell suspensions were seeded in six-well ultralow attachment plates (Corning) at a density of 5,000 cells/mL in complete MammoCult Medium (Stem Cell Technologies). After 7 days, mammosphere cultures were photographed using a phase-contrast microscope (Olympus) and mammospheres $\geq$ 50 μm were counted using ImageJ software (NIH).

Animal studies

Animal protocols were approved by the Johns Hopkins University Animal Care and Use Committee and were in accordance with the NIH Guide for the Care and Use of Laboratory Animals. For tumorigenicity assays, 125 or 250 cells of a MDA-MB-231 subclone were injected into the mammary fat pad (MFP) of 5-to-7 week-old female SCID mice in a 1:1 (vol:vol) suspension of Matrigel (BD Biosciences) in PBS. Seventy days after injection, the number of mice that developed palpable tumors was recorded. For other assays, 2×10^6 MDA-MB-231 parental or knockdown subclone cells, or 2×10^6 SUM-159 knockdown subclone cells, were injected into the MFP of 5-to-7 week-old female SCID mice. Mice were treated with drugs as indicated when tumor volume reached 200 mm^3 (for MDA-MB-231) or 120 mm^3 (for SUM-159). Primary tumors were measured for length (L) and width (W), and tumor volume (V) was calculated as $V = L \times W^2 \times 0.524$.

Bioinformatics and statistical analysis

Expression data for DUSP and HIF target-gene mRNAs in primary breast cancers was accessed from The Cancer Genome Atlas (TCGA) invasive carcinoma gene expression dataset (cancergenome.nih.gov). Pearson test was performed to analyze the correlation of DUSP expression with the HIF metagene signature. Expression of DUSP9 and DUSP16 in primary breast cancer patient dataset GSE12237 was accessed from the Gene Expression Omnibus (ncbi.nlm.nih.gov/geo/). Kaplan–Meier curves were generated using Kaplan-Meier plotter (kmplot.com) and the log-rank test was performed. For tumorigenicity assays, the Fisher exact test was performed. For all other assays, differences between two groups were analyzed by Student *t* test, whereas differences between multiple groups were analyzed by ANOVA with Bonferroni posttest. *P* values < 0.05 were considered significant for all analyses.

Results

Chemotherapy inhibits ERK and activates p38 MAPK signaling through HIF1–mediated reciprocal regulation of *DUSP9* and *DUSP16* gene expression

To investigate the response of MAPK pathways to chemotherapy in TNBC, we treated MDA-MB-231 cells that were stably transduced with lentiviral vector encoding a nontargeting control (NTC) shRNA with paclitaxel or carboplatin for 72 hours at the drug concentration that inhibited growth by 50% (IC_{50}). Each of these drugs inhibited phosphorylation of ERK and stimulated phosphorylation of p38 and JNK (Fig. 1A). shRNA-mediated knockdown of HIF1α, or double knockdown (DKD) of HIF1α and HIF2α but not knockdown of HIF2α alone, abrogated paclitaxel- or carboplatin-mediated ERK inhibition and p38 activation (Fig. 1A), indicating that paclitaxel and carboplatin inhibit ERK and activate p38 signaling in a HIF1α–dependent and HIF2α–independent manner. Chemotherapy-induced JNK activation was not affected by knockdown of HIF1α, HIF2α, or both (Fig. 1A), indicating that chemotherapy activates JNK signaling independent of HIFs.

To investigate whether DUSPs are involved in HIF1–dependent regulation of ERK and p38 MAPK activities in response to chemotherapy, we first compared expression of sixteen DUSP mRNAs with an HIF metagene signature consisting of 10 HIF-regulated mRNAs (ANGPTL4, LDHA, PGK1, CA9, CXCR3, L1CAM, BNIP3, PLOD1, P4HA1, and P4HA2) using data obtained from 1,215 human breast cancers in the TCGA database (31). Expression of DUSP9 and DUSP16 mRNA showed the highest positive and negative correlation with the HIF signature, respectively (Supplementary Fig. S1A). We also compared the expression of DUSP9 and DUSP16 mRNA in different molecular subtypes of breast cancer (Luminal A, Luminal B, HER2-enriched, and Basal) that are based on a 50-mRNA (PAM50) signature (32). In basal breast cancers, the subtype containing most TNBCs and in which HIF target genes are most highly expressed (10, 31), DUSP9 mRNA levels were significantly increased, whereas DUSP16 mRNA levels were significantly decreased, compared with other breast cancer subtypes (Fig. 1B).

To define MAPK substrates of DUSP9 and DUSP16 in TNBC cells, we generated stable DUSP9 and DUSP16 knockdown subclones by transducing MDA-MB-231 cells with a lentiviral expression vector encoding either of two independent shRNAs targeting DUSP9 or DUSP16. MDA-MB-231 NTC, DUSP9-knockdown, or DUSP16-knockdown subclones were treated with paclitaxel and phosphorylation of ERK, p38, and JNK MAPKs was analyzed. Knockdown of DUSP9 abrogated paclitaxel-mediated inhibition of phosphorylation of ERK and the ERK substrate FoxO3, without affecting paclitaxel-induced phosphorylation of p38 and JNK (Fig. 1C, left), indicating that ERK is the substrate of DUSP9 in MDA-MB-231 cells. Knockdown of DUSP16 increased phosphorylation of p38, especially in response to paclitaxel treatment, without affecting paclitaxel-induced changes in the phosphorylation of ERK or JNK, indicating that p38 is the substrate of DUSP16 (Fig. 1C, right).

To examine whether chemotherapy-induced expression of DUSP9 or DUSP16 is HIF regulated, we treated MDA-MB-231 NTC, HIF1α-knockdown, HIF2α-knockdown, or DKD subclones with paclitaxel or carboplatin for 72 hours and found that DUSP9 expression was increased, whereas DUSP16 expression was decreased by paclitaxel or carboplatin treatment in subclones at the mRNA (Fig. 1D) and protein (Fig. 1E) levels. Knockdown of HIF1α, but not of HIF2α, abrogated chemotherapy-induced *DUSP9* expression and *DUSP16* repression. Coadministration of the HIF1 inhibitor digoxin also blocked paclitaxel- or carboplatin-induced *DUSP9* expression and *DUSP16* repression in MDA-MB-231 and in another TNBC cell line, SUM-159 (Supplementary Fig. S1B).

To determine the clinical relevance of DUSP9 and DUSP16 expression in response to chemotherapy, we analyzed a Gene Expression Omnibus dataset (GSE12237), which stratified patients with breast cancer based on whether they received chemotherapy (33), and found that chemotherapy was associated with increased DUSP9 and decreased DUSP16 mRNA expression (Fig. 1F). Taken together, these data indicate that chemotherapy decreases ERK activity through HIF1-dependent expression of *DUSP9* and increases p38 activity through HIF1-dependent repression of *DUSP16* (Supplementary Fig. S2A, S2C, and S2E).

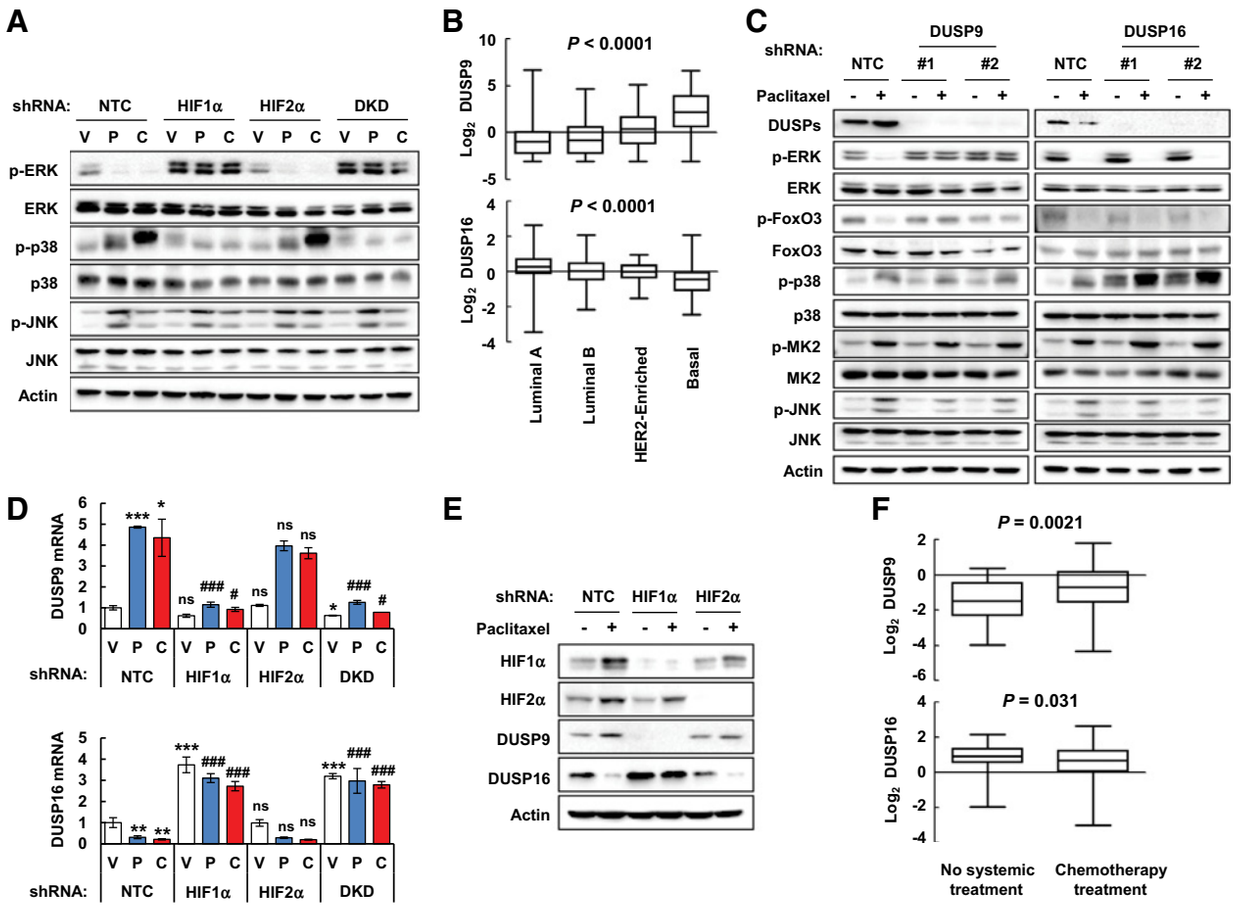

Figure 1.

HIF1 inhibits ERK and stimulates p38 activity through reciprocal regulation of DUSP9 and DUSP16 expression. **A,** MDA-MB-231 subclones, which were stably transduced with vector encoding NTC shRNA or shRNA against HIF1α, HIF2α, or both (DKD), were treated with vehicle (V), 10 nmol/L paclitaxel (P), or 100 μmol/L carboplatin (C) for 72 hours, and immunoblot assays were performed. **B,** Log_2 expression of DUSP9 (top) and DUSP16 (bottom) mRNA from 1,215 human breast cancer specimens in the TCGA database was compared according to molecular subtype (ANOVA with Bonferroni posttest). **C,** MDA-MB-231 subclones, which were stably transduced with expression vector encoding NTC or either of two different shRNAs (#1 and #2) targeting DUSP9 (left) or DUSP16 (right), were incubated without (−) or with (+) 10 nmol/L paclitaxel for 72 hours, and immunoblot assays were performed. **D,** MDA-MB-231 subclones were treated with vehicle, 10 nmol/L paclitaxel, or 100 μmol/L carboplatin for 72 hours, and RT-qPCR assays were performed to analyze DUSP9 and DUSP16 mRNA expression (mean ± SEM; $n = 3$). *, $P < 0.05$; **, $P < 0.01$; ***, $P < 0.001$ vs. NTC/V; #, $P < 0.05$; ###, $P < 0.001$ vs. corresponding NTC subclone; ns, not significant (ANOVA with Bonferroni posttest). **E,** MDA-MB-231 subclones were treated without (−) or with (+) 10 nmol/L paclitaxel for 72 hours, and immunoblot assays were performed. **F,** Log_2 expression of DUSP9 and DUSP16 mRNA in human breast cancers from the GSE12237 dataset in the Gene Expression Omnibus. The data were stratified based on whether the patient received chemotherapy or not, and statistical analysis was performed using Student *t* test.

HIF1 directly activates *DUSP9* and indirectly represses *DUSP16* through REST

To investigate whether HIF1 directly binds to the *DUSP9* gene and activates its transcription, chromatin immunoprecipitation (ChIP) assays were performed in MDA-MB-231 cells to evaluate candidate HIF1 binding sites that matched the consensus sequence 5′-(A/G)CGTG-3′. A DNA sequence located in the 5′-flanking region of the *DUSP9* gene was enriched by ChIP with HIF1α or HIF1β antibodies when cells were exposed to paclitaxel or carboplatin (Fig. 2A), or subjected to hypoxia (Supplementary Fig. S3A), indicating direct binding of HIF1 to the *DUSP9* gene.

Because HIF1 functions as a transcriptional activator, we hypothesized that a transcriptional repressor that is regulated by HIF1 might serve as an intermediate for *DUSP16* repression (34). The repressor element 1-silencing transcription factor (REST) has been reported to mediate hypoxia-induced transcriptional repression (35, 36). We found that in MDA-MB-231 cells, REST mRNA and protein expression was induced in response to paclitaxel or carboplatin treatment, which was abrogated in HIF1α knockdown and DKD, but not HIF2α knockdown, subclones (Fig. 2B and C). Consistently, pharmacological inhibition of HIF1 by digoxin also blocked paclitaxel- or carboplatin-induced *REST* expression (Supplementary Fig. S3B), suggesting that *REST* gene transcription is activated by HIF1 in response to chemotherapy. ChIP analysis performed in MDA-MB-231 cells showed that paclitaxel or carboplatin treatment (Fig. 2D), or hypoxia exposure (Supplementary Fig. S3C) induced the binding of HIF1α and HIF1β to the 5′-flanking region of the *REST* gene, indicating that

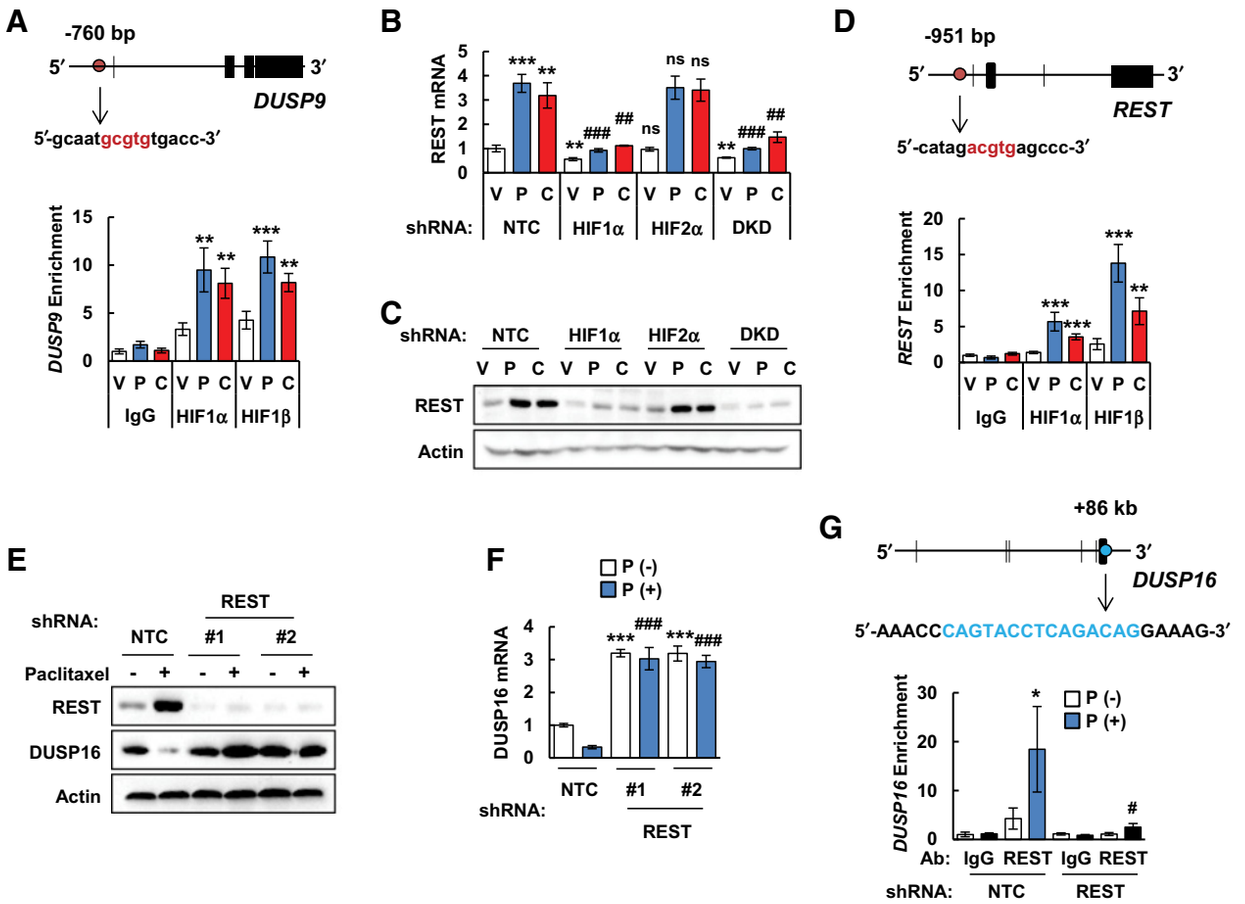

Figure 2.

HIF1 directly activates *DUSP9* transcription and indirectly represses *DUSP16* transcription through REST. **A** and **D,** MDA-MB-231 cells were treated with vehicle (V), 10 nmol/L paclitaxel (P), or 100 μmol/L carboplatin (C) for 72 hours, and ChIP assays were performed using IgG or antibodies against HIF1α or HIF1β. Primers flanking candidate HIF binding sites in the *DUSP9* (**A**) and *REST* (**D**) genes were used for qPCR, and the results were normalized to V/IgG (mean ± SEM; $n = 4$). **, $P < 0.01$; ***, $P < 0.001$ vs. V (ANOVA with Bonferroni posttest). The nucleotide sequence surrounding the HIF1 binding sites (red) in the 5′-flanking region of *DUSP9* (**A**) and *REST* (**D**) is shown. **B** and **C,** MDA-MB-231 subclones were treated with vehicle, paclitaxel, or carboplatin for 72 hours. RT-qPCR (**B**) and immunoblot (**C**) assays were performed (mean ± SEM; $n = 3$). **, $P < 0.01$; ***, $P < 0.001$ vs. NTC/V; ##, $P < 0.01$; ###, $P < 0.001$ vs. corresponding NTC subclone; ns, not significant (ANOVA with Bonferroni posttest). **E** and **F,** MDA-MB-231 subclones, transduced with vector encoding NTC or either of two different shRNAs targeting REST (#1 and #2), were treated without [P(−)] or with [P(+)] 10 nmol/L paclitaxel for 72 hours, and immunoblot (**E**) and RT-qPCR (**F**) assays were performed (mean ± SEM; $n = 3$). ***, $P < 0.001$ vs. NTC/P(−); ###, $P < 0.001$ vs. NTC/P(+) (ANOVA with Bonferroni posttest). **G,** MDA-MB-231 subclones, transduced with vector encoding NTC or REST shRNA, were treated as indicated and ChIP assay was performed using IgG or antibody against REST. The results were normalized to NTC/IgG/P(−) (mean ± SEM; $n = 4$). *, $P < 0.05$ vs. NTC/REST/P(−); #, $P < 0.05$ vs. NTC/REST/P(+) (ANOVA with Bonferroni posttest). The nucleotide sequence surrounding the REST binding site (blue) within exon 6 of the *DUSP16* gene is shown.

REST is a direct HIF1 target gene. REST knockdown abrogated paclitaxel-induced *DUSP16* repression in both MDA-MB-231 (Fig. 2E and F) and SUM-159 (Supplementary Fig. S3D) TNBC cells. In ChIP assays, we identified a REST binding site located within exon 6 of the *DUSP16* gene (Fig. 2G). Binding of REST to this DNA sequence was induced by paclitaxel treatment and was decreased in REST knockdown subclones, validating the specificity of the REST antibody. We also found that expression of RCOR2, a REST corepressor, was induced by paclitaxel or carboplatin treatment in a HIF1–dependent manner (Supplementary Fig. S3E and S3F). HIF1α and HIF1β bound to the 5′-flanking region of *RCOR2* (Supplementary Fig. S3G). However, in both MDA-MB-231 and SUM-159 cells, knockdown of RCOR2 failed to block paclitaxel-mediated *DUSP16* repression (Supplementary Fig. S3H and S3I). Taken together, these data indicate that HIF1 activates *DUSP9* transcription through direct binding and indirectly represses *DUSP16* by activating *REST* gene transcription (Supplementary Fig. S2A and S2B).

DUSP9 and DUSP16 reciprocally regulate chemotherapy-induced BCSC enrichment

To investigate whether DUSP9 and DUSP16 regulate the BCSC phenotype, we cultured MDA-MB-231 and SUM-159 cells as mammospheres, which enriches for BCSCs (37). DUSP9 protein levels were increased, while DUSP16 protein levels were decreased in nonadherent mammosphere cultures as compared with standard monolayer cultures (Fig. 3A). Consistently, ERK was dephosphorylated whereas p38 was phosphorylated in mammosphere

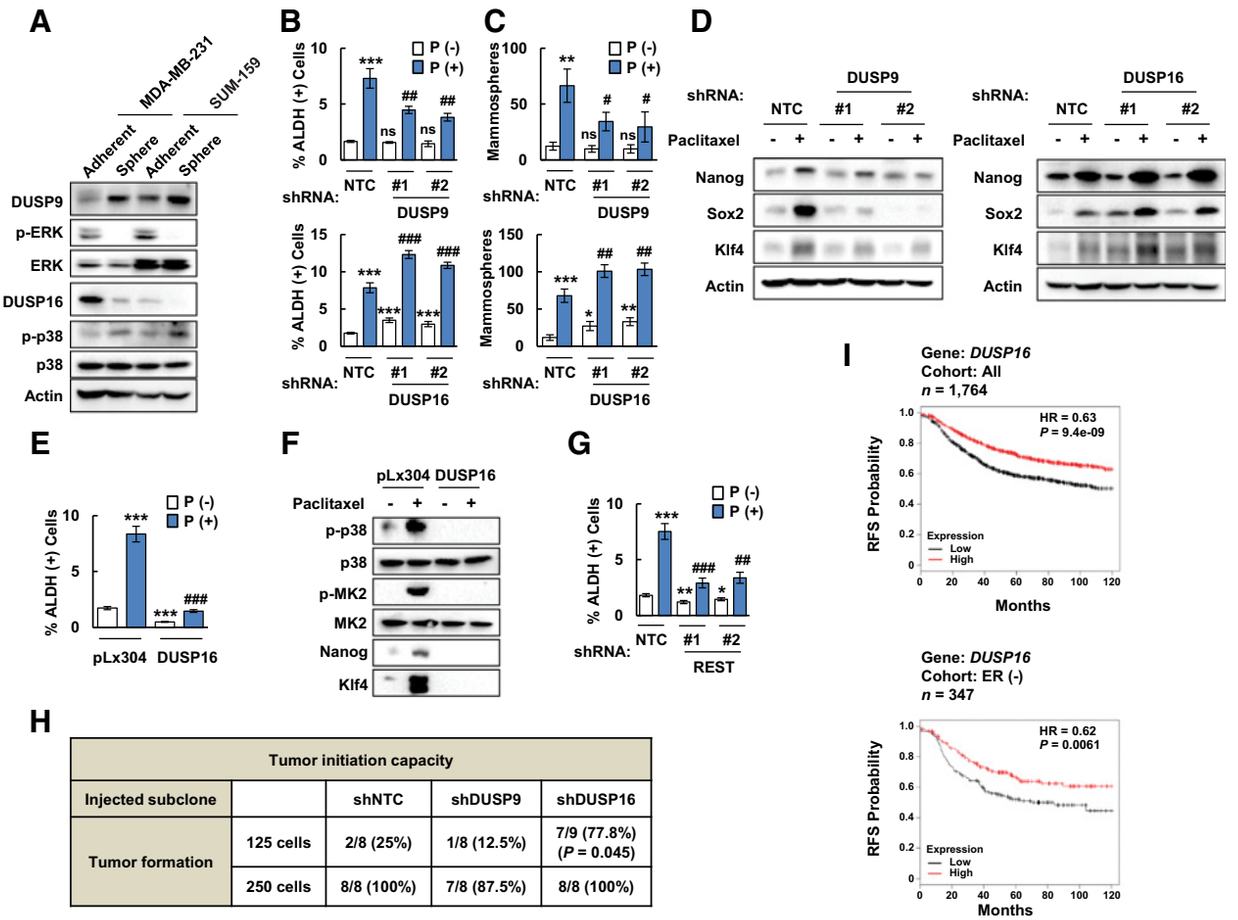

Tumor initiation capacity				
Injected subclone		shNTC	shDUSP9	shDUSP16
Tumor formation	125 cells	2/8 (25%)	1/8 (12.5%)	7/9 (77.8%) (*P* = 0.045)
	250 cells	8/8 (100%)	7/8 (87.5%)	8/8 (100%)

Figure 3.

DUSP9 and DUSP16 reciprocally regulate the BCSC phenotype. **A,** MDA-MB-231 and SUM-159 cells were cultured on standard tissue culture plates (adherent) or ultralow adherence plates (sphere) for 6 days and harvested for immunoblot assays. **B** and **C,** MDA-MB-231 subclones, stably transduced with vector encoding NTC or either of two different shRNAs (#1 and #2) targeting DUSP9 (top) or DUSP16 (bottom), were treated without [P(−)] or with [P(+)] 10 nmol/L paclitaxel for 72 hours, and the percentage of ALDH$^+$ cells (**B**) and the number of mammospheres formed per 1,000 cells seeded (**C**) were determined (mean ± SEM; $n = 3$). *, $P < 0.05$; **, $P < 0.01$; ***, $P < 0.001$ vs. NTC/P(−); $^{\#}$, $P < 0.05$; $^{\#\#}$, $P < 0.01$; $^{\#\#\#}$, $P < 0.001$ vs. NTC/P(+); ns, not significant (ANOVA with Bonferroni posttest). **D,** MDA-MB-231 subclones, stably transduced with vector encoding NTC or shRNA targeting DUSP9 (left) or DUSP16 (right), were cultured without (−) or with (+) 10 nmol/L paclitaxel for 72 hours, and immunoblot assays were performed. **E** and **F,** MDA-MB-231 cells transfected with empty pLx304 vector or vector encoding DUSP16 were incubated without [P(−)] or with [P(+)] 10 nmol/L paclitaxel for 72 hours. The percentage of ALDH$^+$ cells was determined (**E**; mean ± SEM; $n = 3$) and immunoblot assays were performed (**F**). ***, $P < 0.001$ versus pLx304/P(−); $^{\#\#\#}$, $P < 0.001$ vs. pLx304/P(+) (ANOVA with Bonferroni posttest). **G,** MDA-MB-231 subclones transduced with vector encoding NTC or REST shRNA were treated as indicated, and the percentage of ALDH$^+$ cells was determined (mean ± SEM; $n = 3$). *, $P < 0.05$; **, $P < 0.01$; ***, $P < 0.001$ vs. NTC/P(−); $^{\#\#}$, $P < 0.01$; $^{\#\#\#}$, $P < 0.001$ vs. NTC/P(+) (ANOVA with Bonferroni posttest). **H,** MDA-MB-231 subclones expressing the indicated shRNA were implanted into the MFP (125 or 250 cells each). The number of mice that developed a tumor after 10 weeks is shown, and Fisher exact test was performed to determine statistical significance versus NTC (ANOVA with Bonferroni posttest). **I,** Kaplan–Meier analyses of RFS were performed based on clinical and molecular data from patients with breast cancer (cohort: all; top) or from a subgroup of patients with ER (−) breast cancer [cohort: ER (−), bottom]. The patients were stratified according to DUSP16 mRNA levels in the primary tumor, which were greater (red) or less (black) than the median level. The hazard ratio (HR) and *P* value (log-rank test) for each comparison are shown.

cultures, without changes in total protein levels (Fig. 3A). To examine the role of DUSP9 and DUSP16 in chemotherapy-induced BCSC enrichment, MDA-MB-231 NTC, DUSP9-, or DUSP16-knockdown subclones were treated with paclitaxel for 72 hours and subjected to the mammosphere assay or assayed for ALDH activity, which also identifies populations of cells that are enriched for BCSCs (38). DUSP9 knockdown inhibited paclitaxel-induced enrichment of ALDH$^+$ cells and mammosphere-forming cells (Fig. 3B and C), indicating that DUSP9 expression is required for chemotherapy-induced BCSC enrichment. DUSP16 knockdown increased the percentage of ALDH$^+$ cells and number of mammosphere-forming cells and further promoted paclitaxel-mediated BCSC induction (Fig. 3B and C), indicating that DUSP16 inhibits chemotherapy-induced BCSC enrichment. The role of DUSP9 and DUSP16 in the regulation of chemotherapy-induced enrichment of ALDH$^+$ cells was confirmed in SUM-159 cells (Supplementary Fig. S4A).

Paclitaxel treatment also induced expression of the pluripotency factors Nanog, Sox2, and Klf4 in MDA-MB-231 cells, which was attenuated by DUSP9 knockdown and was potentiated

by DUSP16 knockdown (Fig. 3D). Overexpression of DUSP16 in MDA-MB-231 and SUM-159 cells, which completely dephosphorylated p38 (Supplementary Fig. S4B), abrogated paclitaxel-induced enrichment of $ALDH^+$ cells (Fig. 3E; Supplementary Fig. S4C) and blocked pluripotency factor expression (Fig. 3F). Consistently, knockdown of REST, which increased *DUSP16* expression (Fig. 2F), also blocked paclitaxel-induced enrichment of $ALDH^+$ cells (Fig. 3G; Supplementary Fig. S4D) and pluripotency factor gene expression (Supplementary Fig. S4E) in both MDA-MB-231 and SUM-159 TNBC cells.

To investigate the role of DUSP9 and DUSP16 in regulating the tumorigenic capacity of TNBC cells *in vivo*, we injected 125 or 250 cells of the MDA-MB-231 NTC, DUSP9-, or DUSP16-knockdown subclone into the MFP of female SCID mice (Fig. 3H). With injection of 125 cells, 2 of 8 mice (25%) formed tumors in the NTC group 10 weeks after injection, whereas DUSP16 knockdown cells showed significantly increased tumor-initiating capacity with tumor formation in 7 of 9 mice (78%), supporting the role of DUSP16 in the inhibition of BCSC maintenance. DUSP9 knockdown did not significantly decrease tumor-initiating capacity after injection of either 125 or 250 cells. This result was consistent with the *in vitro* results demonstrating that DUSP9 knockdown did not significantly decrease the percentage of $ALDH^+$ cells or the number of mammosphere-forming cells in the absence of paclitaxel treatment (Fig. 3B and C).

To investigate the clinical relevance of DUSP16 and DUSP9 expression with regard to patient survival, we analyzed DUSP16 mRNA levels in 1,764 primary breast cancers of all subtypes (Fig. 3I, top) or 347 breast cancers that were ER-negative (Fig. 3I, bottom) and found that DUSP16 mRNA levels greater than the median were associated with increased relapse-free survival (RFS) in both cohorts. DUSP9 mRNA expression was not a prognostic factor for RFS in patients with breast cancer (Supplementary Fig. S4F). Taken together, these data demonstrate the reciprocal roles of DUSP9 and DUSP16 in the regulation of chemotherapy-induced BCSC enrichment (Supplementary Fig. S2B–S2E).

p38 promotes paclitaxel-induced BCSC enrichment through phosphorylation of ZFP36L1

Previously, we showed that paclitaxel induces inhibition of MEK-mediated ERK activity, leading to dephosphorylation and nuclear localization of FoxO3, transcriptional activation of *Nanog*, and BCSC enrichment (11). In the current study, we focused on the role of the DUSP16–p38 axis in the specification of BCSCs in response to chemotherapy. Pharmacological inhibition of p38 activity by SB203580 blocked paclitaxel-induced expression of the pluripotency factors Nanog, Sox2, and Klf4 in MDA-MB-231 cells (Fig. 4A) and abrogated the paclitaxel-induced increase in the percentage of $ALDH^+$ cells in both MDA-MB-231 (Fig. 4B) and SUM-159 (Supplementary Fig. S5A) cells, indicating that p38 catalytic activity is required for paclitaxel-mediated BCSC enrichment.

We next investigated the mechanism by which p38 regulates pluripotency factor expression and the BCSC phenotype. It has been reported that p38 stimulates FoxO3 nuclear localization in response to doxorubicin treatment in the ER^+ breast cancer cell line MCF-7 (39). However, in MDA-MB-231 cells, inhibition of p38 by treatment with SB203580 failed to block paclitaxel-induced FoxO3 nuclear translocation (Supplementary Fig. S5B). Because p38 can regulate downstream gene expression by transcriptional or posttranscriptional mechanisms, we measured Nanog and Klf4 mRNA stability after p38 inhibition. MDA-MB-231 and SUM-159 cells were treated without or with p38 inhibitor for 24 hours and global mRNA transcription was inhibited by treatment with flavopiridol (40) or actinomycin D (41). The degradation of existing Nanog and Klf4 mRNA was monitored by RT-qPCR at different time points after inhibition of mRNA synthesis. In both MDA-MB-231 and SUM-159 cells, the half-life of Nanog and Klf4 mRNA was decreased by more than 50% (Fig. 4C; Supplementary Fig. S5C). These data suggest that p38 posttranscriptionally regulates Nanog and Klf4 expression by mRNA stabilization.

Next, we searched for RNA-binding proteins (RBP), which regulate mRNA stability, and found that paclitaxel treatment induces phosphorylation of zinc finger protein 36 C3H type-like 1 (ZFP36L1; Fig. 4D), which leads to its inactivation (42). Cotreatment with the p38 inhibitor SB203580, or PF3644022, which is an inhibitor of the p38 substrate MAPK-activated protein kinase 2 (MK2), blocked paclitaxel-induced phosphorylation of ZFP36L1 (Fig. 4D), leading to degradation of Nanog and Klf4 mRNA. Consistently, knockdown of ZFP36L1 expression in MDA-MB-231 (Fig. 4E) and SUM-159 (Supplementary Fig. S5D) cells increased basal levels of Nanog and Klf4 mRNA and potentiated paclitaxel-induced Nanog and Klf4 mRNA expression (Fig. 4F; Supplementary S5E).

To investigate whether p38 regulates the BCSC phenotype through a similar mechanism *in vivo*, we implanted MDA-MB-231 cells in the MFP of female SCID mice and treated the mice with saline, paclitaxel (10 mg/kg on days 0, 5, and 10), p38 inhibitor LY2228820 (10 mg/kg on days 0–13), or the combination of paclitaxel and LY2228820, starting when tumors reached a volume of 200 mm^3 (day 0). Tumor volume was measured every 2 to 3 days (Fig. 5A), and tumors were harvested on day 13 for analysis of $ALDH^+$ (Fig. 5B) and mammosphere-forming (Fig. 5C) cells, the phosphorylation of MK2 and ZFP36L1, and the expression of Nanog and Klf4 (Fig. 5D). Although p38 inhibition alone failed to inhibit tumor growth significantly, the combination of paclitaxel and LY2228820 had a greater inhibitory effect on tumor growth compared with either drug alone (Fig. 5A). LY2228820 abrogated paclitaxel-induced increases in $ALDH^+$ (Fig. 5B) and mammosphere-forming (Fig. 5C) cells and expression of Nanog and Klf4 (Fig. 5D), indicating inhibition of the BCSC phenotype. LY2228820 also blocked paclitaxel-induced phosphorylation of ZFP36L1 (Fig. 5D). Taken together, these data indicate that p38–MK2 signaling stabilizes Nanog and Klf4 mRNA through phosphorylation and inactivation of ZFP36L1 in response to paclitaxel, leading to enrichment of BCSCs (Supplementary Fig. S2F– S2H).

Chemotherapy promotes BCSC enrichment through HIF1–regulated DUSP9 and DUSP16 expression *in vivo*

To investigate the role of DUSP9 and DUSP16 in chemotherapy-induced BCSC enrichment *in vivo*, 2×10^6 MDA-MB-231 (Fig. 6A–C) or SUM-159 (Supplementary Fig. S6A and S6B) NTC, DUSP9-, or DUSP16-knockdown subclone cells were implanted into the MFP of female SCID mice, and when the tumor volume reached 200 mm^3 (MDA-MB-231) or 120 mm^3 (SUM-159), the mice were treated with 10 mg/kg of paclitaxel by intraperitoneal injection every 5 days for three doses. Tumors were harvested 3 days after the last dose and subjected to ALDH, mammosphere, and immunoblot assays. Paclitaxel increased the percentage of $ALDH^+$ cells, the number of mammosphere-forming cells, and

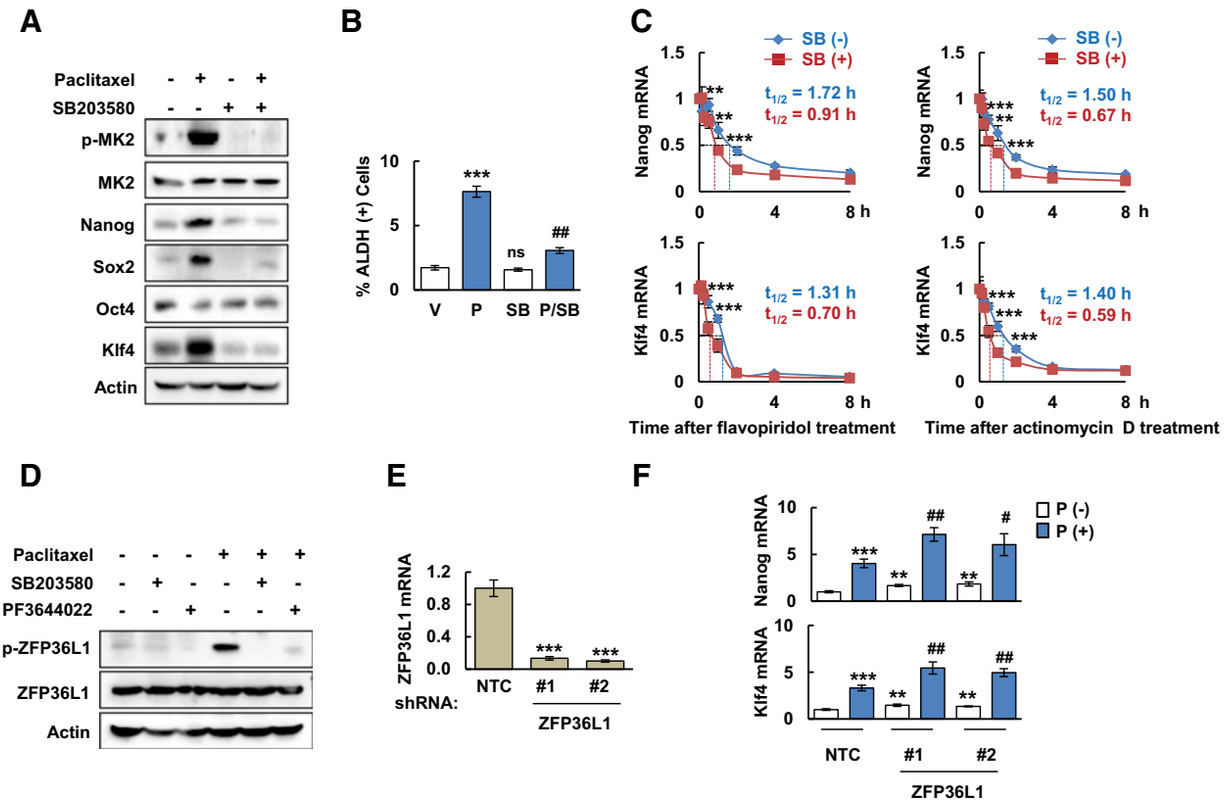

Figure 4.

p38 MAPK regulates the BCSC phenotype through posttranscriptional regulation of pluripotency factor mRNAs. **A** and **B,** MDA-MB-231 cells were treated with vehicle (V), 10 nmol/L paclitaxel (P), 5 μmol/L SB203580 (SB), or the combination (P/SB) for 72 hours, and immunoblot (**A**) and ALDH (**B**) assays were performed (mean ± SEM; $n = 3$). ***, $P < 0.001$ vs. V; ##, $P < 0.01$ vs. P; ns, not significant (ANOVA with Bonferroni posttest). **C,** MDA-MB-231 cells were incubated without [SB(−)] or with [SB(+)] 5 μmol/L SB203580 for 24 hours to inhibit p38 activity, and then were treated with 0.8 μmol/L flavopiridol for 3 hours (left) or 2 μmol/L actinomycin D for 4 hours (right) to block transcription. Nanog and Klf4 mRNA levels were determined by RT-qPCR at the indicated time points (mean ± SEM; $n = 3$). **, $P < 0.01$; ***, $P < 0.001$ vs. SB(−) (ANOVA with Bonferroni posttest). Half-life of Nanog and Klf4 mRNA is indicated by the dotted lines. **D,** MDA-MB-231 cells were treated with 10 nmol/L paclitaxel, alone or in combination with 5 μmol/L SB203580 or 200 nmol/L PF3644022, for 72 hours, and immunoblot assays were performed. **E,** MDA-MB-231 cells were transfected with vector encoding NTC or either of two different shRNAs (#1 and #2) targeting ZFP36L1 and RT-qPCR was performed (mean ± SEM; $n = 3$). ***, $P < 0.001$ vs. NTC (ANOVA with Bonferroni posttest). **F,** MDA-MB-231 subclones transfected with vector encoding NTC or ZFP36L1 shRNA were treated as indicated and RT-qPCR was performed (mean ± SEM; $n = 3$). **, $P < 0.01$; ***, $P < 0.001$ vs. NTC/P(−); #, $P < 0.05$; ##, $P < 0.01$ vs. NTC/P(+) (ANOVA with Bonferroni posttest).

Nanog and Klf4 protein levels, and this effect was attenuated by DUSP9 knockdown and potentiated by DUSP16 knockdown (Fig. 6A–C; Supplementary Fig. S6A and S6B). Paclitaxel induced DUSP9 expression and decreased phosphorylation of its substrate ERK, whereas DUSP9 knockdown abrogated paclitaxel-induced ERK dephosphorylation. Paclitaxel also inhibited DUSP16 expression and increased phosphorylation of its substrate p38, and DUSP16 knockdown further increased paclitaxel-induced p38 phosphorylation (Fig. 6C).

To confirm the role of HIF1 in the reciprocal regulation of DUSP9 and DUSP16 *in vivo* and to further explore the clinical implications of our findings, we investigated the effect of pharmacological inhibition of HIF1 with digoxin, administered in combination with carboplatin, another chemotherapy drug that is used to treat TNBC. Mice injected with MDA-MB-231 cells were treated with vehicle, carboplatin (20 mg/kg every 5 days for 3 doses), digoxin (2 mg/kg daily), or the combination of carboplatin and digoxin. Previously, we showed that coadministration of digoxin inhibited the carboplatin-induced increase in $ALDH^+$ cells and mammosphere-forming cells *in vivo* (11). Here, we consistently found that digoxin, which completely inhibited HIF1α expression, abrogated carboplatin-induced expression of Nanog and Klf4 (Fig. 6D). Carboplatin induced DUSP9 expression, ERK dephosphorylation, REST expression, DUSP16 repression, and p38 phosphorylation, all of which were abrogated by coadministration of digoxin. The effects of digoxin administration *in vitro* (Supplementary Figs. S1B and S3B) and *in vivo* (Fig. 6D) were similar to those caused by shRNA-mediated HIF1α-knockdown *in vitro* (Fig. 1A, D and E, and Fig. 2B and C). Taken together, these data (Supplementary Fig. S2A, S2C, and S2E) indicate that HIF1–regulated DUSP9 and DUSP16 signaling pathways mediate chemotherapy-induced BCSC enrichment in TNBC.

Discussion

BCSCs are resistant to chemotherapy, and the percentage of BCSCs is further increased in response to chemotherapy, which

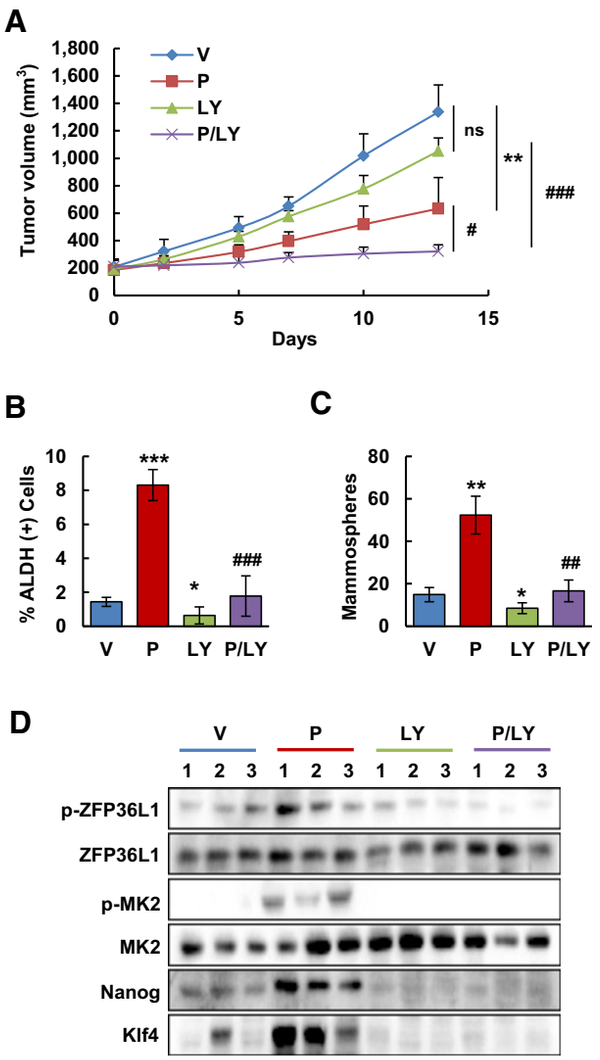

Figure 5.

Inhibition of p38 blocks tumor growth, paclitaxel-induced pluripotency factor expression, and BCSC enrichment *in vivo*. MDA-MB-231 cells were implanted into the MFP of female SCID mice. When tumor volume reached 200 mm^3 (day 0), mice were randomly assigned to four groups, which were treated with vehicle (V), paclitaxel (P; 10 mg/kg by intraperitoneal injection on days 0, 5, and 10), LY2228820 (LY; 10 mg/kg by oral gavage on days 0–13), or the combination (P/LY). Tumor volume was determined every 2–3 days (**A**; mean ± SEM; $n = 3$). **, $P < 0.01$; #, $P < 0.05$; ###, $P < 0.001$; ns, not significant. Tumors were harvested from the MFP on day 13 for ALDH (**B**), mammosphere (**C**), and immunoblot (**D**) assays (mean ± SEM; $n = 3$). *, $P < 0.05$; **, $P < 0.01$; ***, $P < 0.001$ vs. V; ##, $P < 0.01$; ###, $P < 0.001$ vs. P (ANOVA with Bonferroni posttest).

contributes to breast cancer recurrence and metastasis. Previous studies have demonstrated that HIFs play a critical role in chemotherapy-induced BCSC enrichment (10–12). In the present study, we have demonstrated that HIF1 reciprocally regulates DUSP9 and DUSP16 expression in response to chemotherapy, leading to inactivation of ERK and activation of p38 MAPK signaling pathways. Both inactivation of ERK signaling, which increases transcription of genes encoding pluripotency factors, and activation of p38, which stabilizes mRNA encoding pluripotency factors, mediate induction of the BCSC phenotype. Thus, HIF1 is an upstream regulator of MAPK activity through direct and indirect regulation of *DUSP9 a*nd *DUSP16* transcription (Fig. 6E). Similar results were observed in MDA-MB-231 TNBC cells, which are *KRAS*-mutant, and SUM-159 TNBC cells, which are *KRAS*-wild type.

The MAPK pathways are commonly dysregulated in breast cancer and are associated with aggressive phenotypes, such as increased cell proliferation and resistance to apoptosis (43). Although MAPK kinases (such as MEK), which phosphorylate and activate MAPKs, are considered as potential targets for breast cancer treatment, most kinase inhibitors have failed in clinical trials due to the complexity of signaling networks containing feedback loops and cross-talk with other pathways (44). Computational analysis suggested that the extent of MAPK phosphorylation is dictated by DUSPs rather than MAPK kinases, highlighting the critical role of DUSPs as the control point of MAPK signaling networks (45). Unlike the MAPK kinases, the activity of which is regulated by phosphorylation, the phosphatases are constitutively active and regulated at the level of gene expression. Here, we report that two DUSPs, DUSP9 and DUSP16, are reciprocally regulated by the same transcription factor, HIF1, through different molecular mechanisms. *DUSP9* transcription is directly activated by HIF1, whereas *DUSP16* is indirectly repressed by HIF1 through its activation of *REST* gene transcription. HIF1–dependent activation of DUSP9 and inactivation of DUSP16 in response to chemotherapy cause inactivation of ERK and activation of p38, respectively, both of which lead to increased expression of the pluripotency factors Nanog and Klf4, and enrichment of BCSCs. Interestingly, inactivation of ERK and activation of p38 increase pluripotency factor expression by different modes: inactivation of ERK causes dephosphorylation and activation of FoxO3, which activates *Nanog* transcription (11), whereas activation of p38 leads to stabilization of Nanog and Klf4 mRNA through phosphorylation and inactivation of ZFP36L1. These results demonstrating multimodal regulation of ERK and p38 activity by HIF1 stand in contrast to the conventional paradigm in which MAPKs function as upstream regulators of transcription factors.

RBPs are important regulators of mRNA stability through binding to the 3′ untranslated regions of mRNAs (46). ZFP36L1 is an RBP that has been reported to regulate mouse embryonic stem cell fate through binding to mRNAs encoding pluripotency factors including Nanog (47). Here, we found that ZFP36L1 is phosphorylated and inactivated by the p38 substrate MK2, leading to stabilization of Nanog and Klf4 mRNA in TNBC cells. However, the mechanism underlying inactivation of ZFP36L1 is not clear. Whether phosphorylation of ZFP36L1 decreases its ability to bind to target mRNAs or affects the recruitment of mRNA-degrading enzymes needs to be determined in future studies. The p38 pathway has been implicated in the regulation of several other RBPs in different contexts, including TTP, ZFP36L2, KSRP, and HuR, all of which are involved in determining the stability of mRNA transcripts (48). Further studies are warranted to determine whether these RBPs cooperate to regulate pluripotency factor mRNAs and the BCSC phenotype.

Our results suggest that ERK may not be a good therapeutic target in combination with chemotherapy for the treatment of TNBC, because inhibition of ERK will enrich for BCSCs (11), whereas activation of ERK will promote bulk cancer cell

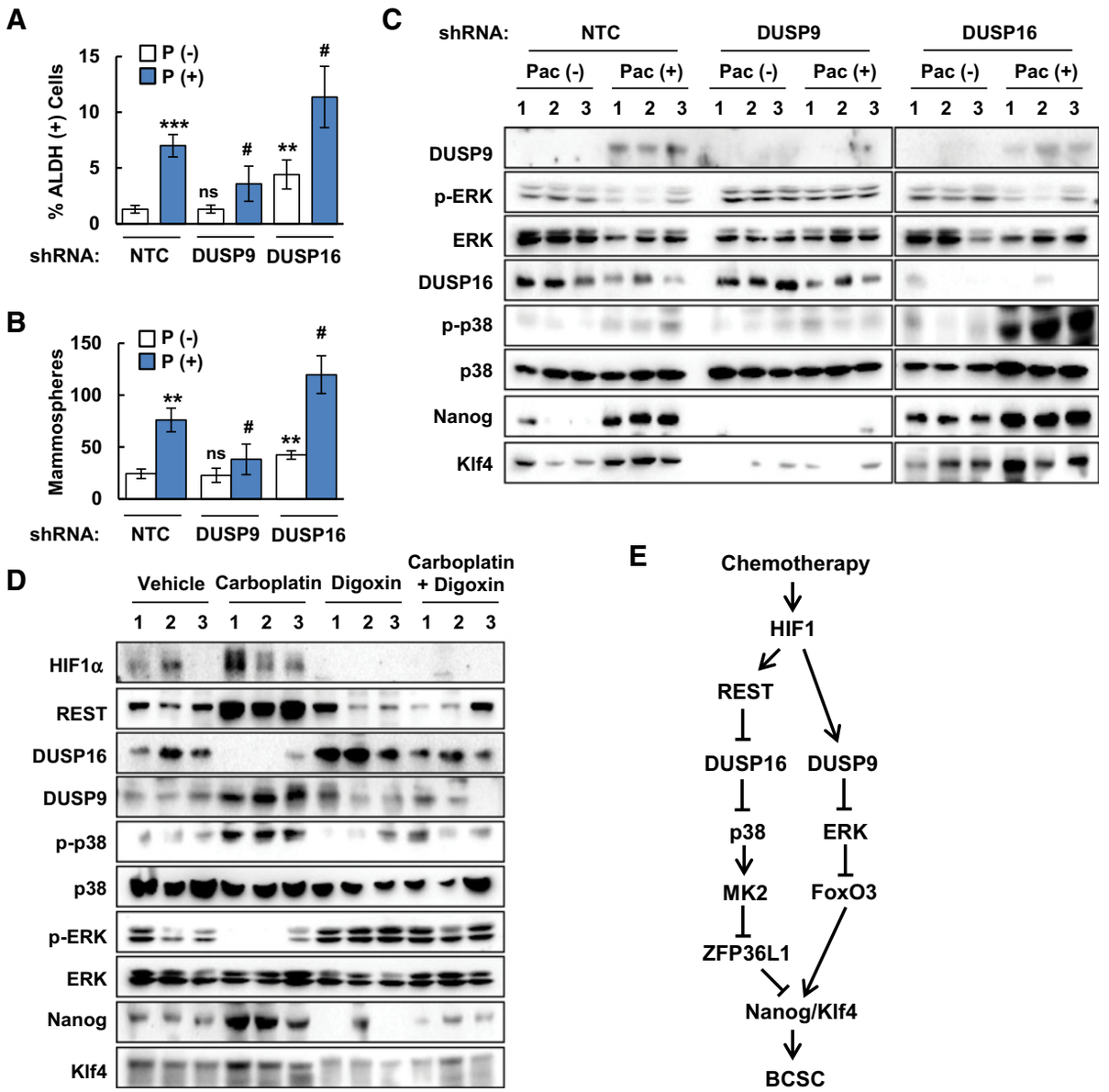

Figure 6.

Chemotherapy regulates HIF1–dependent DUSP9 and DUSP16 expression, leading to pluripotency factor expression and BCSC enrichment *in vivo*. **A–C,** 2×10^6 cells of MDA-MB-231 subclones were implanted into the MFP of female SCID mice. When tumor volume reached 200 mm^3 (day 0), mice were grouped randomly and treated with saline [P(−)] or 10 mg/kg paclitaxel [P(+)] on days 0, 5, and 10. Tumor samples were harvested on day 13 for ALDH (**A**), mammosphere (**B**), and immunoblot (**C**) assays. **, $P < 0.01$; ***, $P < 0.001$ vs. NTC/P(−); $^{\#}$, $P < 0.05$ vs. NTC/P(+); ns, not significant (ANOVA with Bonferroni posttest). **D,** MDA-MB-231 cells were implanted into the MFP. When tumor volume reached 200 mm^3 (day 0), mice were randomly assigned to four groups, which were treated with vehicle, carboplatin (20 mg/kg i.p. on days 0, 5, and 10), digoxin (2 mg/kg i.p. on days 0–13), or the combination of carboplatin and digoxin. Tumor samples were harvested on day 13 for immunoblot assays. **E,** Chemotherapy reciprocally regulates HIF1–dependent DUSP9 and DUSP16 expression and mediates ERK inhibition and p38 activation, respectively, leading to increased expression of pluripotency factors and BCSC enrichment.

proliferation (49), neither of which is desired. In contrast, we have demonstrated that inhibition of p38 not only sensitizes breast cancer cells to paclitaxel treatment, but also abrogates paclitaxel-induced BCSC enrichment *in vivo*, implicating p38 inhibition as a potential strategy to target BCSCs. The p38 inhibitors LY2228820 (ralimetinib) and LY3007113 are currently in clinical trials for the treatment of breast cancer and other solid tumors (50, 51). More detailed studies are warranted to evaluate the efficacy of p38 inhibitors, especially in combination with chemotherapy, in the eradication of BCSCs.

BCSCs must evade the innate and adaptive immune systems in order to form a recurrent or metastatic tumor. Our current work is focused on the intrinsic mechanisms for BCSC specification in response to chemotherapy. One caveat of the study is

that the study of orthotopic tumors in immunodeficient mice excludes the role of the immune system. We recently reported that chemotherapy induces the expression of CD47, CD73, and PDL1 in a HIF-dependent manner, enabling TNBC cells to evade killing by macrophages and cytotoxic T lymphocytes (52). Additional *in vivo* studies using immunocompetent models are warranted to determine whether ERK inactivation or p38 activation in TNBC cells also promotes immune evasion in response to chemotherapy.

An alternative approach to block chemotherapy-induced BCSC enrichment is by inhibition of HIF1. Although the results of a phase I trial of a HIF2 inhibitor in patients with kidney cancer have been reported (53), no drug that directly targets HIF1 has reached clinical trials. In our current and previous studies, we have demonstrated that genetic or pharmacological inhibition of HIF1 blocks chemotherapy-induced enrichment of cells with BCSC (10–12) and immune evasive (52) properties *in vivo* through multiple mechanisms. Taken together, these studies provide compelling evidence that coadministration of an HIF1 inhibitor with cytotoxic chemotherapy may be a particularly effective means to inhibit BCSC enrichment and improve patient survival in TNBC.

Disclosure of Potential Conflicts of Interest

No potential conflicts of interest were disclosed.

Authors' Contributions

Conception and design: H. Lu, I. Chen, G.L. Semenza
Development of methodology: H. Lu, L. Tran
Acquisition of data (provided animals, acquired and managed patients, provided facilities, etc.): H. Lu, L. Tran, Y. Park, J. Lan
Analysis and interpretation of data (e.g., statistical analysis, biostatistics, computational analysis): H. Lu, I. Chen, J. Lan, Y. Xie, G.L. Semenza
Writing, review, and/or revision of the manuscript: H. Lu, G.L. Semenza
Administrative, technical, or material support (i.e., reporting or organizing data, constructing databases): G.L. Semenza
Study supervision: G.L. Semenza

Acknowledgments

We thank Karen Padgett of Novus Biologicals for providing antibodies listed in Supplementary Table S3. G.L. Semenza is an American Cancer Society Research Professor and the C. Michael Armstrong Professor at the Johns Hopkins University School of Medicine. This work was supported by Breast Cancer Research Program Impact Award W81XWH-12-0464 from the Department of Defense, Research Professor Award RP-16-239-06-COUN from the American Cancer Society, and a grant from the Cindy Rosencrans Foundation (all to G.L. Semenza).

The costs of publication of this article were defrayed in part by the payment of page charges. This article must therefore be hereby marked *advertisement* in accordance with 18 U.S.C. Section 1734 solely to indicate this fact.

Received January 26, 2018; revised May 8, 2018; accepted June 1, 2018; published first June 7, 2018.

References

1. Foulkes WD, Smith IE, Reis-Filho JS. Triple-negative breast cancer. N Engl J Med 2010;363:1938–48.
2. Ovcaricek T, Frkovic SG, Matos E, Mozina B, Borstnar S. Triple negative breast cancer - prognostic factors and survival. Radiol Oncol 2011; 45:46–52.
3. Twelves C, Jove M, Gombos A, Awada A. Cytotoxic chemotherapy: still the mainstay of clinical practice for all subtypes metastatic breast cancer. Crit Rev Oncol Hematol 2016;100:74–87.
4. Al-Hajj M, Wicha MS, Benito-Hernandez A, Morrison SJ, Clarke MF. Prospective identification of tumorigenic breast cancer cells. Proc Natl Acad Sci U S A 2003;100:3983–8.
5. Li X, Lewis MT, Huang J, Gutierrez C, Osborne CK, Wu MF, et al. Intrinsic resistance of tumorigenic breast cancer cells to chemotherapy. J Natl Cancer Inst 2008;100:672–9.
6. Charafe-Jauffret E, Ginestier C, Iovino F, Wicinski J, Cervera N, Finetti P, et al. Breast cancer cell lines contain functional cancer stem cells with metastatic capacity and a distinct molecular signature. Cancer Res 2009;69:1302–13.
7. Creighton CJ, Li X, Landis M, Dixon JM, Neumeister VM, Sjolund A, et al. Residual breast cancers after conventional therapy display mesenchymal as well as tumor-initiating features. Proc Natl Acad Sci U S A 2009;106: 13820–5.
8. Pece S, Tosoni D, Confalonieri S, Mazzarol G, Vecchi M, Ronzoni S, et al. Biological and molecular heterogeneity of breast cancers correlates with their cancer stem cell content. Cell 2010;140:62–73.
9. Bhola NE, Balko JM, Dugger TC, Kuba MG, Sánchez V, Sanders M, et al. TGF-β inhibition enhances chemotherapy action against triple-negative breast cancer. J Clin Invest 2013;123:1348–58.
10. Samanta D, Gilkes DM, Chaturvedi P, Xiang L, Semenza GL. Hypoxia-inducible factors are required for chemotherapy resistance of breast cancer stem cells. Proc Natl Acad Sci U S A 2014;111:E5429–38.
11. Lu H, Samanta D, Xiang L, Zhang H, Hu H, Chen I, et al. Chemotherapy triggers HIF-1-dependent glutathione synthesis and copper chelation that induces the breast cancer stem cell phenotype. Proc Natl Acad Sci U S A 2015;112:E4600–9.
12. Lu H, Chen I, Shimoda LA, Park Y, Zhang C, Tran L, et al. Chemotherapy-Induced Ca2+ release stimulates breast cancer stem cell enrichment. Cell Rep 2017;18:1946–57.
13. Pazarentzos E, Bivona TG. Adaptive stress signaling in targeted cancer therapy resistance. Oncogene 2015;34:5599–606.
14. Keyse SM.Dual-specificity MAP kinase phosphatases (MKPs) and cancer. Cancer Metastasis Rev 2008;27:253–61.
15. Haagenson KK, Wu GS. The role of MAP kinases and MAP kinase phosphatase-1 in resistance to breast cancer treatment. Cancer Metastasis Rev 2010;29:143–9.
16. Pearson G, Robinson F, Beers Gibson T, Xu BE, Karandikar M, Berman K, et al. Mitogen-activated protein (MAP) kinase pathways: regulation and physiological functions. Endocr Rev 2001;22:153–83.
17. Kondoh K, Nishida E. Regulation of MAP kinases by MAP kinase phosphatases. Biochim Biophys Acta 2007;1773:1227–37.
18. Jeffrey KL, Camps M, Rommel C, Mackay CR. Targeting dual-specificity phosphatases: manipulating MAP kinase signalling and immune responses. Nat Rev Drug Discov 2007;6:391–403.
19. Huang CY, Tan TH. DUSPs, to MAP kinases and beyond. Cell Biosci 2012;2:24.
20. Brondello JM, Brunet A, Pouysségur J, McKenzie FR. The dual specificity mitogen-activated protein kinase phosphatase-1 and -2 are induced by the p42/p44MAPK cascade. J Biol Chem 1997;272:1368–76.
21. Ryser S, Massiha A, Piuz I, Schlegel W. Stimulated initiation of mitogen-activated protein kinase phosphatase-1 (MKP-1) gene transcription involves the synergistic action of multiple cis-acting elements in the proximal promoter. Biochem J 2004;378:473–84.
22. Ekerot M, Stavridis MP, Delavaine L, Mitchell MP, Staples C, Owens DM, et al. Negative-feedback regulation of FGF signalling by DUSP6/MKP-3 is driven by ERK1/2 and mediated by Ets factor binding to a conserved site within the DUSP6/MKP-3 gene promoter. Biochem J 2008;412:287–98.
23. Wang J, Ford HR, Grishin AV. NF-kappaB-mediated expression of MAPK phosphatase-1 is an early step in desensitization to TLR ligands in enterocytes. Mucosal Immunol 2010;3:523–34.
24. Bermudez O, Jouandin P, Rottier J, Bourcier C, Pagès G, Gimond C. Post-transcriptional regulation of the DUSP6/MKP-3 phosphatase by MEK/ERK signaling and hypoxia. J Cell Physiol 2011;226:276–84.
25. Hou PC, Li YH, Lin SC, Lin SC, Lee JC, Lin BW, et al. Hypoxia-induced downregulation of DUSP-2 phosphatase drives colon cancer stemness. Cancer Res 2017;77:4305–16.

26. Semenza GL. Hypoxia-inducible factors in physiology and medicine. Cell 2012;148:399–408.
27. Schito L, Semenza GL. Hypoxia-inducible factors: master regulators of cancer progression. Trends Cancer 2016;2:758–70.
28. Choudhry H, Harris AL. Advances in hypoxia-inducible factor biology. Cell Metab 2018;27:281–98.
29. Cao Y, Eble JM, Moon E, Yuan H, Weitzel DH, Landon CD, et al. Tumor cells upregulate normoxic HIF-1α in response to doxorubicin. Cancer Res 2013;73:6230–42.
30. Zhang H, Wong CC, Wei H, Gilkes DM, Korangath P, Chaturvedi P, et al. HIF-1-dependent expression of angiopoietin-like 4 and L1CAM mediates vascular metastasis of hypoxic breast cancer cells to the lungs. Oncogene 2012;31:1757–70.
31. The Cancer Genome Atlas Network. Comprehensive molecular portraits of human breast tumors. Nature 2012;490:61–70.
32. Parker JS, Mullins M, Cheang MC, Leung S, Voduc D, Vickery T, et al. Supervised risk predictor of breast cancer based on intrinsic subtypes. J Clin Oncol 2009;27:1160–7.
33. Bos PD, Zhang XH, Nadal C, Shu W, Gomis RR, Nguyen DX, et al. Genes that mediate breast cancer metastasis to the brain. Nature 2009;459:1005–9.
34. Feige E, Yokoyama S, Levy C, Khaled M, Igras V, Lin RJ, et al. Hypoxia-induced transcriptional repression of the melanoma-associated oncogene MITF. Proc Natl Acad Sci U S A 2011;108:E924–33.
35. Cavadas MA, Cheong A, Taylor CT. The regulation of transcriptional repression in hypoxia. Exp Cell Res 2017;356:173–81.
36. Cavadas MA, Mesnieres M, Crifo B, Manresa MC, Selfridge AC, Keogh CE, et al. REST is a hypoxia-responsive transcriptional repressor. Sci Rep 2016;6:31355.
37. Dontu G, Abdallah WM, Foley JM, Jackson KW, Clarke MF, Kawamura MJ, et al. In vitro propagation and transcriptional profiling of human mammary stem/progenitor cells. Genes Dev 2003;17:1253–70.
38. Ginestier C, Hur MH, Charafe-Jauffret E, Monville F, Dutcher J, Brown M, et al. ALDH1 is a marker of normal and malignant human mammary stem cells and a predictor of poor clinical outcome. Cell Stem Cell 2007;1:555–67.
39. Ho KK, McGuire VA, Koo CY, Muir KW, de Olano N, Maifoshie E, et al. Phosphorylation of FOXO3a on Ser-7 by p38 promotes its nuclear localization in response to doxorubicin. J Biol Chem 2012;287:1545–55.
40. Batista PJ, Molinie B, Wang J, Qu K, Zhang J, Li L, et al. m(6)A RNA modification controls cell fate transition in mammalian embryonic stem cells. Cell Stem Cell 2014;15:707–19.
41. Perry RP, Kelley DE. Inhibition of RNA synthesis by actinomycin D: characteristic dose-response of different RNA species. J Cell Physiol 1970;76:127–39.
42. Schmidlin M, Lu M, Leuenberger SA, Stoecklin G, Mallaun M, Gross B, et al. The ARE-dependent mRNA-destabilizing activity of BRF1 is regulated by protein kinase B. EMBO J 2004;23:4760–9.
43. Wang D, Boerner SA, Winkler JD, LoRusso PM. Clinical experience of MEK inhibitors in cancer therapy. Biochim Biophys Acta 2007;1773:1248–55.
44. Neuzillet C, Tijeras-Raballand A, de Mestier L, Cros J, Faivre S, Raymond E. MEK in cancer and cancer therapy. Pharmacol Ther 2014;141:160–71.
45. Bhalla US, Ram PT, Iyengar R. MAP kinase phosphatase as a locus of flexibility in a mitogen-activated protein kinase signaling network. Science 2002;297:1018–23.
46. Matoulkova E, Michalova E, Vojtesek B, Hrstka R. The role of the 3' untranslated region in post-transcriptional regulation of protein expression in mammalian cells. RNA Biol 2012;9:563–76.
47. Tan FE, Elowitz MB. Brf1 posttranscriptionally regulates pluripotency and differentiation responses downstream of Erk MAP kinase. Proc Natl Acad Sci U S A 2014;111:E1740–8.
48. Schoenberg DR, Maquat LE. Regulation of cytoplasmic mRNA decay. Nat Rev Genet 2012;13:246–59.
49. Roberts PJ, Der CJ. Targeting the Raf-MEK-ERK mitogen-activated protein kinase cascade for the treatment of cancer. Oncogene 2007;26:3291–310.
50. Patnaik A, Haluska P, Tolcher AW, Erlichman C, Papadopoulos KP, Lensing JL, et al. A first-in-human phase I study of the oral p38 MAPK inhibitor, Ralimetinib (LY2228820 dimesylate), in patients with advanced cancer. Clin Cancer Res 2016;22:1095–102.
51. Goldman JW, Rosen LS, Tolcher AW, Papadopoulos K, Beeram M, Shi P, et al. Phase 1 and pharmacokinetic study of LY3007113, a p38 MAPK inhibitor, in patients with advanced cancer. Invest New Drugs 2017. doi: 10.1007/s10637-017-0532-2.
52. Samanta D, Park Y, Ni X, Li H, Zahnow CA, Gabrielson E, et al. Chemotherapy induces enrichment of CD47+/CD73+/PDL1+ immune evasive triple-negative breast cancer cells. Proc Natl Acad Sci U S A 2018;115:E1239–48.
53. Courtney KD, Infante JR, Lam ET, Figlin RA, Rini BI, Brugarolas J, et al. Phase I dose-escalation trial of PT2385, a first-in-class hypoxia-inducible factor-2α antagonist in patients with previously treated advanced clear cell renal cell carcinoma. J Clin Oncol 2018;36:867–74.